THE MEASUREMENTS OF VEHICLE GLOW ON THE SPACE SHUTTLE

S. B. Mende

Lockheed Palo Alto Research Laboratory

Palo Alto, CA, 94304

P. M. Banks

STAR Laboratory/SEL

Stanford University

Stanford, CA 94305

R. Nobles

Lockheed Palo Alto Research Laboratory

Palo Alto, CA, 94304

O.K. Garriott, and J. Hoffman

Johnson Space Center

Houston, TX

15 March 1983

(NASA-TM-85360) THE MEASUREMENTS OF VEHICLE GLOW ON THE SPACE SHUTTLE (NASA) 39 p
HC A03/MF A01 CSCL 22B

N83-30509

Unclas
G3/18 13098

ABSTRACT

From the combined data set of glow observations on STS-3, STS-4 and STS-5 some of the properties of the shuttle glow were observed. Comparison of the STS-3 (240 km) and STS-5 (305 km) photographs show that the intensity of the glow is about a factor of 3.5 brighter on the low altitude (STS-3) flight. The orbiter was purposely rotated about the x axis in an experiment on STS-5 to observe the dependence of the intensity on the angle of incidence between the spacecraft surface normal and the velocity vector. For a relatively large angle between the velocity vector and the surface normal there is an appreciable glow, provided the surface is not shadowed by some other spacecraft structure. As the angle becomes less the glow intensifies. The grating experiments (STS-4 photography only, STS-5 image intensifier photography) provided a preliminary low resolution spectra of the spacecraft glow. Accurate wavelength calibrations of the STS-5 instrument permitted measuring of the spectrum and intensity of the earth's airglow.

Comparisons with prior airglow measurements provides a great deal of confidence regarding the glow intensities obtained in the experiment and also provide an indication of the intensity of the vehicle glow. Absolute intensity calibration of the instrument was also performed by means of a laboratory standard source. Within the spectral bandwidth of the experiment the dominant airglow line is the (0,0) atmospheric band of O_2. The limb intensity of this line is of the order of 100-300 kilorayleighs (e.g., Megill et al. 1970). Other prominent features are the 5577 line of atomic oxygen and the OH emission bands. The intensity of all of these agrees with previous measurements and with limb intensity predictions.

The spectra of the glow measurements on STS-5 were relatively poor due to the large angle between the velocity vector and the glowing surfaces. Furthermore, the weak first order spectrum of the vehicle glow was superimposed on the bright earth's airglow. Nevertheless, a weak spectra was obtained which shows a spectrally uniform intensity. The photographic densities due to this glow were measured and compared to the absolute intensity measurements. This glow amounted to a few hundred Rayleighs per Angstrom with a spectrum rising towards the infrared. This rise in intensity was not detected directly but rather is an interpretation of the apparent spectrally uniform photographic spectrum combined with the responsivity of the device which is falls rapidly in sensitivity towards the infrared. The integrated amount of vehicle glow emission in the passband of the instrument was of the order of several hundred kilorayleighs.

INTRODUCTION

The apparent vehicle glow of the space shuttle was detected during the flight of STS-3 (Banks, et al. 1983). Although the shuttle glow was not specifically predicted in advance of the flight, it has now been associated with other spacecraft glow which has been shown to surround free flier satellites such as the Atmospheric Explorer (See Torr 1983, Yee and Abreu 1983). Specific investigation of the shuttle glow was started on STS-4 when a transmission grating was mounted in front of a photographic camera and several exposures were taken on orbit to make preliminary spectral measurements (Mende et al. 1983). The STS-4 experiment yielded a single 400 second exposure photograph with glow spectral information. This image, obtained with

relatively poor aspect with respect to the flowing atmospheric ___?, showed that the glow was observed predominantly in the far red to infrared region (6300-8000A) of the instrumental band pass (4300 - 8000A).

From the STS-4 investigation it was evident that the intensity of the glow was reduced for the higher altitude flights (STS-4 was at an altitude of 300 km whereas STS-3 was at 240 km) and that relative insensitivity of unaided photography would seriously limit the spectral glow investigations. Because of this on STS-5 a second instrument was instrument, an image intensified camera, which made the low intensity spectral components of the glow detectable.

THE PERFORMANCE OF THE IMAGE INTENSIFIER ON STS-5

The image intensifier obtained for the STS-5 flight was made and delivered in a fully packaged configuration by VARO Inc. Garland, Texas under the tradename of Noctron 5. This device includes a 25 mm diameter second generation (micro-chanel-plate) image intensifier, a power supply with two AA size batteries, a coupling lens, and adapter rings for 35 mm cameras. Since the 35 mm camera type used on the orbiter was a NIKON we used the NIKON bayonett type adapter rings were employed. With these rings a conventional NIKON camera could be converted simply by including the NOCTRON 5 between the lens and the camera body. A special hood and camera bracket was used to mount the camera in the port side aft flight deck window in the shuttle. The starboard aft flight deck window was used for a conventional Hasselblad camera with the 100 mm focal length lens at F/3.5. For the image intensified NIKON photography the standard 55 mm focal length F/1.4 objective was used in front of the image intensifier.

The image intensifier was a new item for space flight and its suitability for the shuttle flight environment had to be carefully evaluated. Several optical tests were also performed on the device prior to flight. The imaging qualities of the device were evaluated by taking photographs of the night sky and of familiar objects in darkness. Looking through the view finder of the 35 mm camera it could be used as a night vision aid, and relatively high intensity pictures could be obtained under starlit scene conditions. Using a laboratory standard light source and a spectral filter it was established that a one second exposure generated fairly good density when the source brightness was equivalent to 400 Rayleighs. At full gain one could see scintillations with the naked eye due to individual photoelectron emissions from the photocathode through the view finder. However, these scintillations could not be recorded on film. The dark current performance of the device was particularly impressive. With the lens cap on, exposures of 10 seconds did not cause any noticeable increase in film density. The image intensifier unit itself was not subjected to flight qualification testing, because a similar unit had already been qualified for the subsequent April 1983 STS-6 flight. All experiment hardware was stowed in stowage lockers during take off and landing.

THE DEPENDENCE OF THE GLOW INTENSITY ON THE ANGLE OF THE VELOCITY VECTOR

Examination of the earlier glow photographs from STS-3 showed that only those surfaces which were in the direction of the velocity vector exhibited the glow phenomena. An example of such a photograph is given on Figure 1a. Figure 1a and Figure 1b are the comparison of two similar pictures from STS-3 and STS-5 respectively. In both of these photographs the velocity vector is

pointing essentially from the port side in the upper hemisphere (Photographs taken looking aft toward the vertical stabilizer and engine pod structures).

One of the objectives of the STS-5 experiment was to verify that the glow intensity depends solely on the attitude of the surface with respect to the velocity vector, and not on such parameters such as the length of time during which the shuttle was in the night side of the orbit, the amount of residue present on the photo-excited surfaces, or the amount of materials present due to venting or jet firings. It was also desirable to investigate, if possible, the dependence of the glow intensity on the angle of the velocity vector and the surface normal exhibiting the glow luminosity.

These objectives were achieved by the performance of the following experiment. During a nightside pass a full > 360 degree roll was executed about the shuttle x axis while the orbital velocity vector was approximately in the shuttle y-z plane. (Conventional shuttle coordinate system puts the x axis forward toward the nose, the y axis out of the starboard wing and the z axis straight down through the floor of the payload bay.) During the experiment photographic sequences were taken of the vertical stabilizer at 2 minute intervals to record the intensity of the glow on the stabilizer surfaces as a function of the direction of the velocity vector. Sequences consisted of three exposures taken with the image intensifier with durations of 4 sec, 1 sec, and 1/4 sec, respectively. Simultaneously, photographs were taken with the unintensified Hasselblad camera which was mounted in the other aft flight deck window. Of these only the longest (100 second) exposure from this camera gave acceptable photographic densities. However, during this long exposure the attitude changed considerably making the interpretation almost impossible. Thus, only the intensified images have been used in the analysis.

The shortest (the 1/4 second) exposure produced the best intensified glow images and hence these were used to obtain the results which are presented in Figure 2.

The roll experiment started just prior to the taking of the first picture at 16 hours and 33 minutes Mission Elapsed Time (MET). The velocity vector at this time is out of the port and upward directions as shown by the arrow on Figure 2a. Two minutes later at 16:35 the shuttle has rolled and the velocity vector is now essentially at about 35 degrees above the -y axis (port wing). This can be verified because one can see the shadowing caused by the engine pod on the port side. At 16:37 the velocity vector dipped below the horizontal (x y plane) at about 50 degrees and there is only a faint glow remaining on the port side of the stabilizer. The picture taken at 16:37 and 16:39 show no glow at all because the velocity vector is from the bottom up and all the surfaces to be photographed were shadowed and the 16:41 picture shows glow on the upper portion of the starboard side of the stabilizer where it was just coming out of the shadow of the starboard engine pod.

On each image of Figure 2 the approximate direction of the velocity vector is indicated. The direction of the velocity vector was first calculated from orbiter data provided by the Johnson Space Center. The time code on each picture is accurate only to within a minute and therefore the accurate value of the direction of the velocity vector for each photograph had to be interpolated from the position of the stars. By using the frame taken at 16:35 MET (Fig 2.b.) one can establish the direction of the velocity vector fairly accurately from the shadowing of the engine pod. By comparison with the Smithonian Astrophysical Observatory Star Atlas one can establish the rotation

angle with respect to the stars for each exposure and the rotation angle for each exposure in the star coordinate system. Since the velocity vector was essentially in the y-z plane the rotation of the stars gave a fairly accurate value for the angle of the velocity vector. Corrections had to be made for the change of the direction of the velocity vector due to the orbital motion, which amounted to approximately 4 degrees per minute.

The relative magnitude of the glow intensity could be obtained by microdensitometering of the original negative films. Using the original negatives of the images presented on Fig. 1 tracings were made to measure the density of the glow luminosity on the tail section. This density was turned into equivalent exposure and the results are presented on Table 1.

Table 1

THE RELATIVE INTENSITY OF THE STS-5 STABILIZER GLOW

Time Code	Net relative exposure	Side	Angle of velocity to surface normal	Cosine of angle
13:16:33	38	Port	80 deg.	.174
13:16:35	89	Port	28 deg.	.88
13:16:37	tail in shadow		-50 deg.	
13:16:39	tail in shadow		-97 deg.	
13:16:41	113	STBD	29 deg.	.87

Unfortunately, there are not enough data points to draw very solid conclusions. However, the numbers support the type of qualitative conclusions one was able to draw from the pictures. The system was calibrated density versus exposures and from the measured density the net relative exposure or

intensity was derived. The intensity of the glow is not strictly proportional to the cosine of the angle and therefore not strictly proportional to the flux of incoming atmospheric constituents. It appears that very large angles between the surface normals and the velocity vector provide substantial glow. For example, in frame 13:16:33 the angle is 80 degrees to the port side of the tail. When the angle decreases to 28 degrees the increase in glow is just a little over a factor of two. It would seem that the glow detected in the last frame (13:16:41) is anomalously too bright when compared to frame taken at 13:16:35. However, the explanation is clear when one examines the actual photographs of Figure 2. The glow on the starboard side is viewed tangentially, presenting a much narrower and therefore brighter profile than on the portside where the glow is visible over a larger region of the tail surface. If one were to integrate the glow over the larger region no doubt the overall intensity would be of the same order as the more tangential view of the starboard side for the same velocity vector incidence angle. The comparison between the two sides is clearly dependent on the detailed geometry of the problem and we have not sufficient data to pursue this in greater detail.

THE COMPARISON OF THE STS-3 AND STS-5 GLOW INTENSITIES

The glow was discovered by the analysis of the STS-3 photographs. On STS-4 a grating was used in front of the camera to obtain the spectra of the glow but no grating pictures were taken for intensity comparisons. Nevertheless, it was suspected that the intensity of the glow was substantially lower on STS-4 than on STS-3. The altitude of STS-4 and 5 was close to 300 kms whereas the altitude of STS-3 was 240 km. If the glow were

proportional to the density of atomic O one would expect to see a difference of approximately a factor of three in glow intensity due to altitude. On STS-5 the Hasselblad camera sequence was repeated in order to generate pictures for intensitie comparisons with those of STS-3.

A relatively good comparison is provided in Figure 1 where we present an STS-3 and an STS-5 photographs are presented side by side. In these pictures the direction of the velocity vectors are similar.

Both photographs were taken by the same type of camera, a Hasselblad and with the same type of lens (F 3.5). Both negative originals were processed similarly and a control exposure wedge was used to obtain the exposure density curve of each flight film. On the STS-3 picture there are other light sources on the pallet besides the glow. Nevertheless, the glow is clearly visible on the side of the tail section and port side engine pod.

From the comparison of the two photographs of Figure 1. One can see that the glow generated density is roughly the same. This was confirmed by taking a microdensitometer trace of both images using the original negatives. However, the exposure duration for the STS-3 and STS-5 photographs were 10 and 100 seconds, respectively. This suggests a brightness ratio of the order of 10. In reality, however, the films exhibit reciprocity failure and the equivalent exposure is not directly proportional to the exposure time. Using data supplied by the Johnson Space Center (courtesy of Noel Lamar) correction was made for the film reciprocity failure to obtain the real ratio of the glow intensities. The best estimate of the real intensity ratio between the STS-3 and STS-5 glow is about 3.5. This value is consistant with the decrease in

atomic oxygen density for neutral gas pressure between the STS-3 and STS-5 flight altitudes.

WAVELENGTH CALIBRATION

To obtain an accurate wavelength scale it is necessary to take account of several facts. Theoretically, the wavelength is only approximately proportional to the displacement of the image. In practice, both the lens and the image intensifier are likely to exhibit some geometric distortion. To minimize these errors calibration photographs were taken of a slit illuminated by a mercury lamp. For these test exposures the image intensifier camera system was in its full flight configuration. These images were microdensitometered to obtain the displacement due to each mercury line. The following mercury lines could be identified; 4047, 4358.4, 4916, 5460.7, and 5790.7. Another line seen in the infrared was assumed to be the second order of 4047, thus equivalent to 8094 angstroms. To fit the best function for wavelength in terms of displacement a least square fit technique was used where the wavelength y is a function of x according to a simple power law:

$$y = a_0 + a_1 \times X + a_2 \times x^2 + \ldots a_n \times x^n.$$

The fitting was performed for the simple linear case where n=1, the quadratic case and the cubic case. The higher orders naturally gave progressively smaller for residual error square sums. The results are indicated in Table 2.

Table 2

LEAST SQUARE FITS OF WAVELENGTH VERSUS DISPACEMENT-FROM ZERO ORDER

n	1 (linear)	2 (quadratic)	3 (cube)
a0	96.63	-8.260	-.2965
a1	5.183	5.625	4.9869
a2	N/A	-2.933E-2	8.0816E-2
a3	N/A	N/A	4.4871E-5

Table 3

SPECTRAL LINES USED FOR FITTING

Wavelength Å	Displacement Å	1 Å	2 Å	3 Å
0.	0.	96.64	8.26	-.29
4047	762	4046	4107	4070
4358.4	811.	4300	4360	4336
4916	917	4850	4903	4906
5460.7	1022	5394	5434	5461
5790.7	1087	5731	5759	5799
2x4047= 8094	1572	8245	8109	8093
sum of residue squared		47872.05	5832.85	1204.90
"calculated 5577 Å"		5529.45	5564.66	5597.19
best estimate for infrared band		7691.17	7602.94	7629.29

The mercury lines which were used in the least squares fit are shown in Table 3. The displacement of the spectral lines on the film are given in arbitary units as they were measured on the microdensitometer tracing. Columns 1, 2, and 3 refers to the linear, quadratic and cubic fit respectively. The numbers in each column represent the wavelength calculated by substituting the actual displacements into the formulae derived from the least squares fit. From this table it is particularly clear that the higher order fits are becoming rapidly more accurate. This trend is also well demonstrated by the sum of the residue squared as illustrated in Table 3.

An interesting cross check can be found in the calculated value of the 5577 Å line as shown in Table 3. It is interesting to note that the second order fit produces the best agreement.

The main purpose of the spectral calibration was to obtain the wavelength of the infrared emission. Intercomparing the results of the least square fits we can see that the best wavelength estimate is about 7620 + or - 30 angstroms and that the width of the band is of the order of 30 to 40 angstroms. Thus the best candidate for the infrared airglow is the O_2 atmospheric band. This band is not visible from below because of the absorption by the atmospheric O_2. This band is known to be several kilorayleighs in zenith intensity which means that viewed parallel to the Earth limb the emission has an intensity close to 300 kilorayleighs.

ABSOLUTE INTENSITY INTERPRETATIONS

In order to interpret the absolute intensity of the spacecraft glow and the air-glow features it was necessary to take some spectral response calibration exposures. A secondary standard calibration source was used as the test object for these test exposures. The light source contained a quartz halide lamp with ground quartz diffusers to provide an extended source of reasonably spatially uniform emissivity. This lamp was manufactured and calibrated by Prof. R. H. Eather of Boston College. The calibration data plotted in Figure 3 show spectral emissivity in equivalent kilorayleighs per angstrom. The lamp was masked off so that only a .75 in. wide slit was showing and exposures were taken with the image intensifier camera and the grating in position. The resulting streak generated in the dispersion direction was microdensitometered and the density trace is also shown on Figure 3. For completeness sake the shuttle window transmission as provided by the Johnson Space Center is also included in the figure. However, this window was not involved in our calibration test exposures.

To obtain the quantitative response of the image intensifier camera system it was necessary to convert the film density obtained by the microdensitometer into relative exposures. This conversion was obtained by microdensitometering several frames of different exposure times to obtain a relationship between film density and relative exposure. The relative exposure scale was corrected for the film reciprocity. In order to obtain quantitative measurement the of brightness of any feature the observed density of the feature was converted into relative exposure and then compared to the relative exposure obtained using the standard light source. The relative exposure

therefore is an arbitary but linear scale unit. Because of these multiple non-liuear conversions the absolute calibrations are probably no more accurate than 20% to 30%.

The spectral response of the grating intensifier camera device is shown on Figure 4 in relative exposure per kilorayleighs per Angstrom as a function of wavelength.

From the above it can seen that the image intensifier camera system spectral response rises sharply from 4000 Angstroms to about 5400 Angstroms. It is a little puzzling as to why the response is not more uniform towards the blue. Starting above 6500 angstrom the responsivity of the image intensifier is falling off quite rapidly towards the infrared. This is presumably due to the decreased quantum efficiency of its photo cathode.

THE SPECTRA OF THE GLOW

During the STS-4 mission the spectrum of the glow was recorded by an unaided Hasselblad camera using the objective grating (Mende et al., 1983). Based on a single photograph evidence indicated that the spectrum of the glow consisted of a relatively diffuse spectrum primarily at the infrared end of the visible spectrum. Although it was hard to put quantitative numbers on the glow spectrum it seemed to be most intense in the region between 6300 and the window cut off at 8000 angstroms. Because of the lack of sensitivity of the unintensified F/3.5 camera and the unfavorable direction of the velocity vector, a long (400 seconds) exposure duration was required.

On STS-5 the intensified camera permitted the taking of short exposures. Unfortunately the STS-5 spectral results are not useful because the direction of the velocity vector was unfavorable during the time the grating exposures were taken. An additional problem was the presence of the earth near the field of view, producing a strong unwanted background. The clearest example of the glow spectra from STS-5 is on frame 13:17:01, is shown in Figure 5a. Figure 5b is an illustration of the features in the photograph.

The velocity vector in the spacecraft frame of reference at the time of the photograph (illustrated at top of Figure 5b) was 16 degrees to the port from the forward direction and 40 degrees above the bay horizontal. The most intense glow is on the horizontal surfaces such as the top of the engine pods. The zero order image of the tail and pods is in the left half of the picture. The almost vertical slant line cutting through this image is a high order spectral image of the earth limb airglow layer. This is shown as a dashed line on the tracing. The lack of stars shows that the solid earth forms the background for the whole image. Perhaps the clearest first order spectral image is produced by the starboard engine pod. This image is in the center of the picture. The port engine pod is also producing a first order spectrum on the right. They are both illustrated on the tracing.

The relative orientation of the glow on the engine pods and the grating rulings are most unfavorable. The linear wavelength scale was placed against the tip of the zero order starboard engine pod. One can see that the first order image of the shuttle glow seems to occupy a large spectral region from 5000 to 8000 angstrom. The appearance of the first order image is fairly uniform and diffuse showing hardly any spectral features. This appears to

contradict the findings of the STS-4 experiment where we found that the diffuse region only spread between 6300 and 8000. This discrepancy can be resolved by inspecting the absolute value of the glow intensity in Table 4. The image intensifier camera system is much more sensitive in the green region than the film. The marked drop off in the sensitivity of the image intensifier towards the red infrared signifies that the apparently uniform airglow spectra is in reality strongly increasing towards the infrared. On the STS-4 photographs the blue green region was still below the detection threshold and only the more intense infrared end was detectable. Due to the adverse velocity vector angles and the diffuseness of the glow spectra in these pictures microdensitometer tracings did not produce any useful signals.

The device responsivity calibration using the intensity standard permits the interpretation of the various glow features in absolute quantities. The various features and the measured film densities and equivalent relative exposures are given in Table 4.

Table 4

ABSOLUTE CALIBRATION OF VARIOUS GLOW SPECTRA

Frame I.D. (time code)	Feature description	Density (image)	Density (bckgd.)	rel. Exposure (sec)	intensity Rayleighs/ Angstrom
13:17:01 (1/2 sec)	Shuttle glow of stbrd. pod	1.08	.96	.086	(@ 7600A) 850 (@ 7000A) 500 (@ 6000A) 300

The shuttle glow seems to spread through several thousand angstroms so the total integrated amount may be as high as several hundred kilorayleighs in the visible alone.

MEASUREMENT OF AIRGLOW EMISSIONS FROM THE SHUTTLE BASED INTENSIFIER CAMERA

During the performance of the STS-5 glow experiment some images of the earth airglow were obtained, inadvertently, and since the objective grating was in position some excellent spectra of the earth airglow were also obtained. These photographs are the first shuttle based images of this type and are therefore inherently valuable and, in addition, provide excellent calibration to the dispersion and spectral response of the image intensifier camera system.

One such image is illustrated in Figure 6a. As illustrated in the tracing, Fig. 6b, the real or zero order images are on the left. One can clearly see the tail and the two engine pods. The bright line running behind these shuttle features down from left to right is the limb view of the earth's atmosphere. Note that the shuttle is oriented with the bay pointing downward because the image of the solid earth occupies the top right three quarters of the picture. The boundary of the solid earth is faintly visible as illustrated in the tracing of Figure 6b. Several stars zero order (real) images are visible through the earth's atmosphere.

The bright narrow streak first order images of stars show the dispersion direction of the grating. The zero order image of most of these stars are actually outside of the picture. There is one very bright star located between the port engine pod and the tail whose first order spectrum is also visible on the picture.

There are some airglow bands which are parallel to the zero order image of the limb airglow. The first one of these, going from left to right, is the 5577 atomic oxygen recombination glow. This emission is known to be a narrow emission line. Its thickness in first order is due to the altitude extent of the airglow layer. There is a dark band between this and the following wide diffuse region, A most remarkable bright infrared airglow band feature.

The shuttle tail features intersect the airglow layer causing repeated shadows in all the brighter airglow features. Thus there is a tail shadow in 5577 and there is an even more distinct one in the infrared. The edges of the 5577 tail shadow are very sharp showing that the 5577 line is in fact a very narrow spectal feature. Note that the tail being a sharp edge can be regarded as one half of the a spectrometer slit and therefore the resulting intensity change can be interpreted in first order as an accurate measure of the wavelength. This interpretation allows one to make spectral measurements independent of the spatial width of the emitting region. A linear wavelength scale was superimposed on the portside edge of the shadow of the tail section in Figure 6b. The scale confirms that the first shadow is approximately at 5577 and the second shadow is near 8000 Angstroms.

This scale also shows an interesting feature. The scale was carefully drawn parallel with the spectra of the stars to follow the dispersion direction. The scale was also drawn through the intersection of the top of the airglow layer (bottom left on Figures) with the tail section. The scale goes through the corresponding intersection of the tail section with the 5577 image but it is slightly below the corresponding intersection in the infrared image. The explanation is that the infrared airglow layer is displaced in

altitude from the 5577 airglow layer by about 20km. Careful examination of the photograph of Figure 6a shows that the zero order image of the airglow layer consist of two parallel features. This is the most discernable towards the top left part of the zero order image. The double layer of the airglow image can also be seen on other photographs of the limb airglow layer e.g. Banks et al. 1983 Garriott 1979.

The shuttle and the velocity vector duration at the time of the exposure are illustrated at the top of Figure 6b. The velocity vector duration was 15 degrees towards starboard from the forward direction and 25 degrees up in the bay frame of reference. This attitude to the velocity vector is relatively unfavorable from the point of view of strong glow production, but there is some weak glow on the portside engine pod and there are some faint images of the starboard engine pod in first order. These were indicated as dotted images in the Figure.

In Figure 7 the top panel indicates the location of two microdensity traces obtained from the original negative of photograph Figure 6a. The middle panel shows the microdensity trace parallel to the dispersion direction through the tail section shadows. This density trace allows determination of the wavelength scale most accurately. The bottom trace was obtained by tracing perpendicular to the airglow layer. This direction maximizes the signal to noise ratio but distorts the wavelength scale and limits the wave length resolution to the spatial width in the zero order image.

Table 5

THE ABSOLUTE INTENSITY OF THE VARIOUS AIR-GLOW EMISSIONS
(In equivalent Rayleighs/Angstrom)

		Density	Background Density	Exposure		
13:16:55 (1/2 sec)	infrared airglow	1.50	1.17	.56	(@ 7600A)	5000
13:16:55	green airglow	1.25	1.20	.061	(@ 5577A)	200
13:16:55	OH continuum	1.17	.95	.050	(@ 7300A)	300

Note values were obtained by dividing rel. Exposure by device responsitivity (see Fig. 4) as normalized to 1/2 sec exposure.

The intensity values thus obtained agree very well with prior measurements. To compare to prior nonspectral measurements it is necessary to convert these to total intensities in rayleighs within the spectral band of interest.

The infrared airglow is spatial wider than its spectral bandwidth. To interpret the total emission one must refer to the previous measurement of the bandwidth of the feature using the tail shadow. By so doing one obtains roughly 40-60 Angstroms which puts the intensity of the O_2 atmospheric band system to about 300 to 400 kR, in good agreement with previous oblique rocket measurements (Megill et al., 1970).

Since the 5577 is a spectral line feature and its spectral width is very thin the instruments resolution, 20-30 Angstrom, needs to be taken into account. Thus the total measured 5577 intensity is 4000 to 6000 Rayleighs.

The measured intensity of the OH band agrees quite well with other measurements (Broadfoot and Kendall, 1968) of the airglow if we account for the limb view intensification. Thus the spacecraft glow is at least equivalent or brighter than the OH band in limb view.

The intensity of the OH band also agrees quite favorably with the expected limb intensities.

SPACE SHUTTLE BASED IMAGE INTENSIFIER OBSERVATION OF STARS

The space shuttle is a versatile machine which permits the carrying of large astronomical facilities into space. Being above the earth's atmosphere gives several advantages to astronomers. Observations can be made outside the atmospheric window and observations in the atmospheric window can be made without the detremental effects of atmospheric turbulence and diffuse scattering.

Unfortunately the image intensifier observations reported here were made from inside the crew compartment and were made through windows which were coated to prevent transmission of anything except the visible. In any case the purpose of the STS-5 experiment was not to accomplish any astronomical objectives. Nevertheless it is worth discussing the properties of the image intensifier camera system and showing some of the images taken on the STS-5 mission.

The image intensifier camera combination has already been discussed in a previous section. During the first half of the STS-5 glow experiment the

camera was used without the grating and exposures were taken while the shuttle was rolled about its axis to observe the glow intensity change with respect to the velocity vector angle. During the interval while the velocity vector was underneath the payload bay several exposures were made. One of the best such exposures was taken at 13:16:39. This exposure is shown in Figure 8a. The luminosity on the shuttle body is from starlight as the orbiter payload bay is essentially pointing away from the earth.

The starfield in the image is a section of the constellation Pegasus, the declination being a few degrees positive and right ascension around 23 hours. The corresponding section of the Smithonian Astrophysical Observatory star chart is shown in Figure 8b, together with a superimposed outline of the shuttle. By counting the star images in a given area one can identify all the stars presented on the chart. The chart includes stars down to 9th magnitude. This exposure was the shortest (1/4 seconds) of a group of three. Since the shuttle was executing a roll motion during these exposures bluring due to the motion made the other exposures less effective.

The F/1.2 55 mm lens on the image intensifier has an equivalent telescope aperture of about 4.6 cm in diameter. Thus the same image intensifier film combination as a detector and a 46cm (18 in) diameter telescope would detect a 14th magnitude star in a 1/4 second. If a stabilized telescope of this size were to be exposed for 25 seconds the resulting detection threshold would be 19th magnitude. Note that the image tube background seems quite acceptable with this exposure duration. For longer stabilized satellite exposures cooling would be necessary. During a night pass, which has a duration of approximately 2000 seconds, another 3 to 4 orders could be added to the detection threshold.

In other words a modest 18 inch amateur telescope in orbit could rival the largest ground based astronomical telescopes in detection threshold.

In the second half of the glow experiment an objective grating was added to the image intensifier camera combination, thus producing photographic star spectra. For example, the star and its first order spectral image earlier presented in Figure 5a. The best such spectral image was obtained of zeta pegasus. The image density was sufficient to produce a reasonable microdensitometer trace. In Figure 9 the trace of the first order spectra of this object is shown. The trace was actually superimposed on the trace of the background adjacent to the star spectrum. On the same figure the known spectrum of zeta pegasus is also shown (Berger 1976).

Figure 9 shows very clearly the blue and spectral response limitation of the system. Although the spectrum of the star increases towards short wavelengths the response of the intensifier camera system drops off quite sharply above 4000 Angstroms. The spectral transmission of the spacecraft windows, shown earlier in Figure 3, were included in these observations, however, that does not appear to have imposed a limitation.

CONCLUSIONS

From the combined data set of glow observations on STS-3, STS-4 and STS-5 is is possible to define some of the properties of the shuttle glow. Comparison of the STS-3 and STS-5 photographs show that the intensity of the glow is about a factor of 3.5 brighter on the low altitude (STS-3) flight. This result seems to be in good agreement with the ratio of atmospheric

densities between the two altitudes. STS-3 was flown at an altitude of about 240 km whereas STS-5 was flown at an altitude of 305 km. The orbiter was purposely rotated about the x axis in an experiment on STS-5 and the glow was observed. This experiment showed conclusively that the intensity of the glow strongly depends on the angle of incidence between the spacecraft surface and the velocity vector. The relationship, however, does not appear to be a simple cosine law dependence. For a relatively large angle between the velocity vector and the surface normal there is an appreciable glow, provided the surface is not shadowed by some other spacecraft structure. As the angle becomes less the glow intensifies. Unfortunately, the experiment did not provide sufficient data points to express the exact mathematical relationship between the spacecraft glow intensity and the angle between the surface normal and velocity vector.

The grating experiments provided a preliminary low resolution spectra of the spacecraft glow. Accurate wavelength calibrations of the STS-5 instrument allowed a measurement of the spectrum and intensity of the earth's airglow. Comparisons with prior airglow measurements provides confidence regarding the glow intensities obtained in the experiment. Absolute wavelength calibration of the instrument was also performed by means of a laboratory standard source. Within the spectral bandwidth of the experiment the dominant airglow line is the (0,0) band of atmospheric 02. The limb intensity of this line is of the order of 300 kilorayleighs (Megill et al., 1970). Other prominent features are the 5577 line and the OH emission bands. The intensity of all of these well agrees with previous measurements and limb intensity predictions.

The spectra of the glow measurements on STS-5 were relatively unfavorable due to the large angle between the velocity vector and the glowing surfaces and due to the fact that the weak first order spectrum was superimposed on the bright earth's airglow. Nevertheless a weak spectra was obtained which shows a spectrally uniform glow. The photographic densities due to this glow were measured and compared to the absolute intensity measurements. This glow amounted to a few hundred Rayleighs per Angstrom with a spectrum rising towards the infrared. This rise is deduced from an apparent spectrally uniform photographic spectrum combined with the responsivity of the device which is falling rapidly towards the infrared. The integrated amount of light in the passband of the instrument was of the order of several hundred kilorayleighs.

FIGURE CAPTIONS

Figure 1. Unaided Hasselblad photographs on STS-3 and STS-5. The exposure times are 10 and 100 seconds, respectively. The velocity vector is more or less from the same direction for each.

Figure 2. The appearance glow on different parts of the orbiter as the orbiter rotates around the x axis.

Figure 3. The calibration data using the standard light source are plotted in spectral emissivity in equivalent kilorayleighs per angstrom. The calibration exposures were microdensitometered in the dispersion direction. For completeness the shuttle aft flight deck window transmission as provided by the Johnson Space Center is also included. This window was not involved in the calibration test exposures.

Figure 4. The spectral response of the device in relative exposure (arbitary units) per kilorayleighs per Angstrom as a function of wavelength.

Figure 5a. A 1/2 second duration grating exposure of the shuttle tail section with engine pods. The background is the atmospheric airglow emission. Diffuse first order glow spectrum of the engine pods is visible. The faint first order is barely distinguishible from the bright airglow background. The velocity vector is not very favorable to generation of a bright glow emission.

Figure 5b. Tracing of photograph of Figure 5a. Velocity vector direction is indicated on top. Wavelength scale was superimposed on zero and first order images of starboard engine pod.

Figure 6a. The limb view of the earth's airglow through the spectral grating. Image intensified NIKON with 1/2 sec exposure. Objective is F/1.4 55mm. See text and Figure 6b for details.

Figure 6b. Tracing of the photograph of Fig 4a. For explanation see text.

Figure 7. The top panel indicates the two microdensity traces obtained from the original negative of photograph Figure 6a. The center panel shows the microdensity trace parallel to the dispersion direction through the tail section shadows. This density trace allows the most accurate determination of the wavelength scale. The bottom trace was obtained by tracing perpendicular to the airglow layer. This direction maximizes the signal to noise ratio although it distorts the wavelength scale and limits the resolution to the spatial width in the zero order image.

Figure 8a. Starfield taken by image intrensified NIKON F/1.4 1/4 second exposure on TRI-x film.

Figure 8b. The Smithonian Astrophysical Observatory star chart corresponding to the picture of Figure 8a.

Figure 9. The microdensitometer trace of zeta pegazus superimposed on the density trace of the background adjacent to the star spectra. The spectrum of zeta pegasus (Berger M., Catalog of spectrophotometric scans of stars,The Astrophysical Journal Supplement Series, 32, 7-78, 1976) is also shown.

Broadfoot, A .L. and K. R. Kendall, "The airglow spectrum 3100-10,000 angstroms," J. Geophys Res. 73, 426-428, 1968.

Deans, A. J., G. G. Shepherd and W. F. J. Evans, "A rocket measurement of the O2 atmospheric band nightglow altitude distribution," Geophys. Res. Lett., 3, 441-444, 1976.

Garriott, O. K., "Visual observations from space," J. Opt. Soc. Am., 69, 1064-1068, 1979.

Lazarev, A. I., "Optical studies of the emission radiation of the night atmosphere aurora borealis and noctilucent clouds from manned Soviet spacecraft (1961-1981)," Sov. J. Opt. Technol. (USA), Vol.48, no. 4, p. 238-246 (April 1981).

Megill, L. R., A. M. Despain, D. J. Baker and K. D. Baker, "Oxygen atmospheric and infrared atmospheric bands in the aurora," J. Geophys. Res. 75, 4775-4785, 1970.

Packer, D. M., "Altitude of the night airglow radiation," Ann. Geophys., 17, 67-75, 1961.

Tarasova, T. M., "Night-sky emission line intensity distribution with respect to height," Space Res., 3, 162-172, 1963.

Wallace, L. and D. M. Hunten, "Dayglow of the oxygen A band," J. Geophys. Res. 73, 4813-4834, 1968.

Watanabe, T. and M. Nakamura, "Rocket measurements of O2 atmospheric and OH Meinel Bands in the Airglow," J. Geophys. Res. 86, 5768, 1981 (r).

Witt, G., J. Stegman, B. H. Solheim, and E. J. Llewellyn, "A measurement of the O2 atmospheric band and the OI (super 1 S) green line in the nightglow, Planet Space Sci., 27, 341-350, 1979.

STS-3

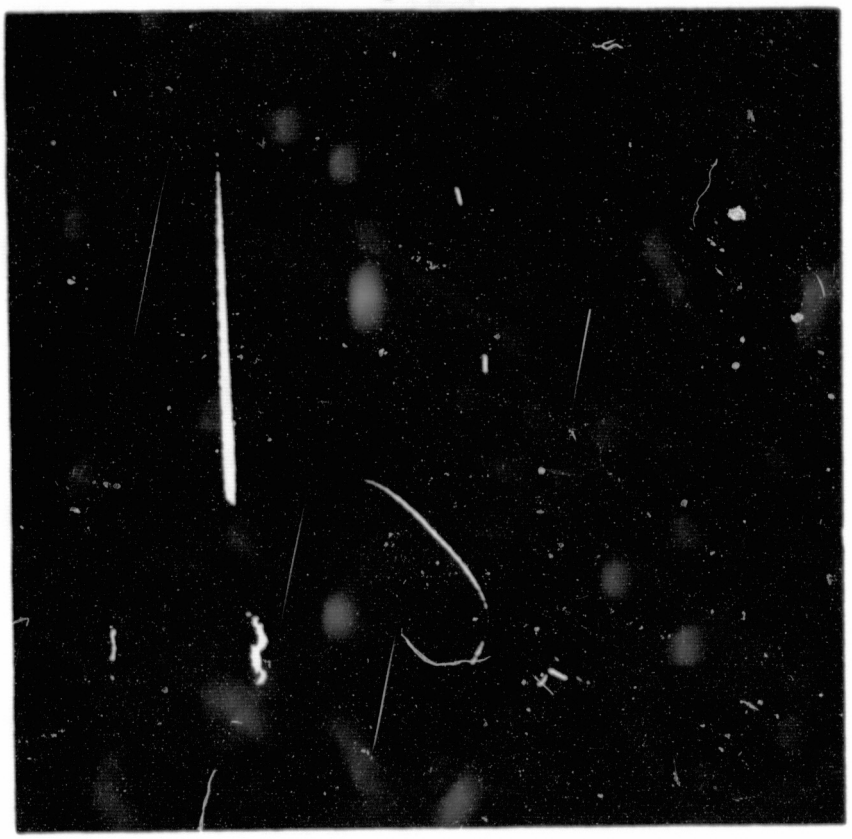

STS-5

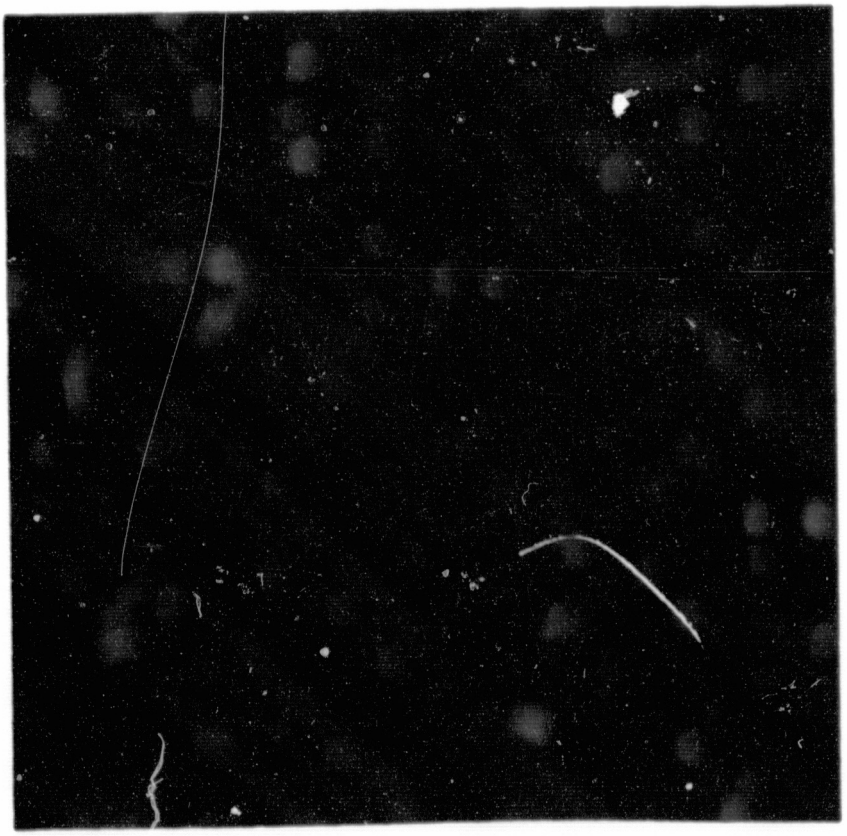

Figure 1.

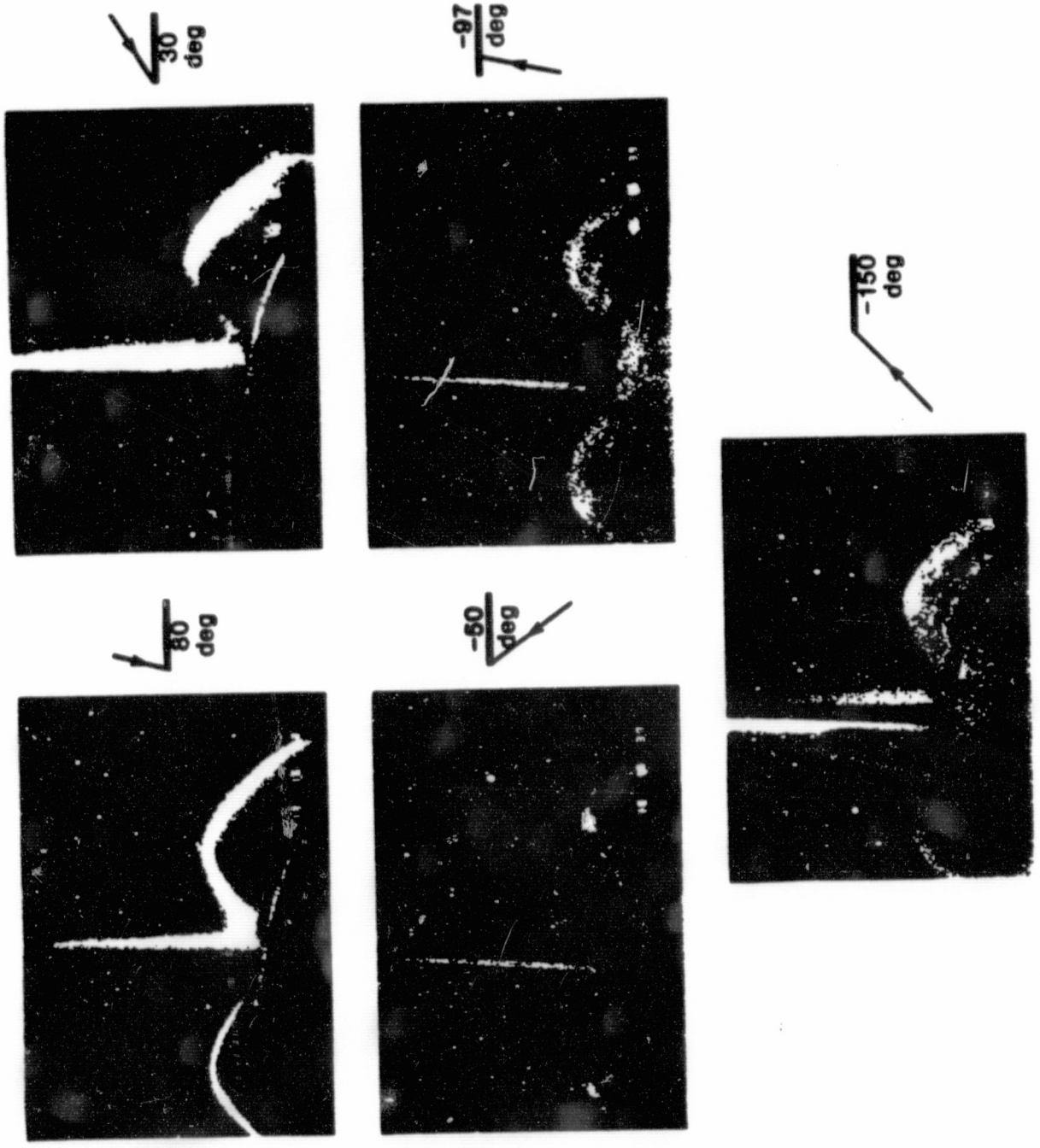

FIGURE 2

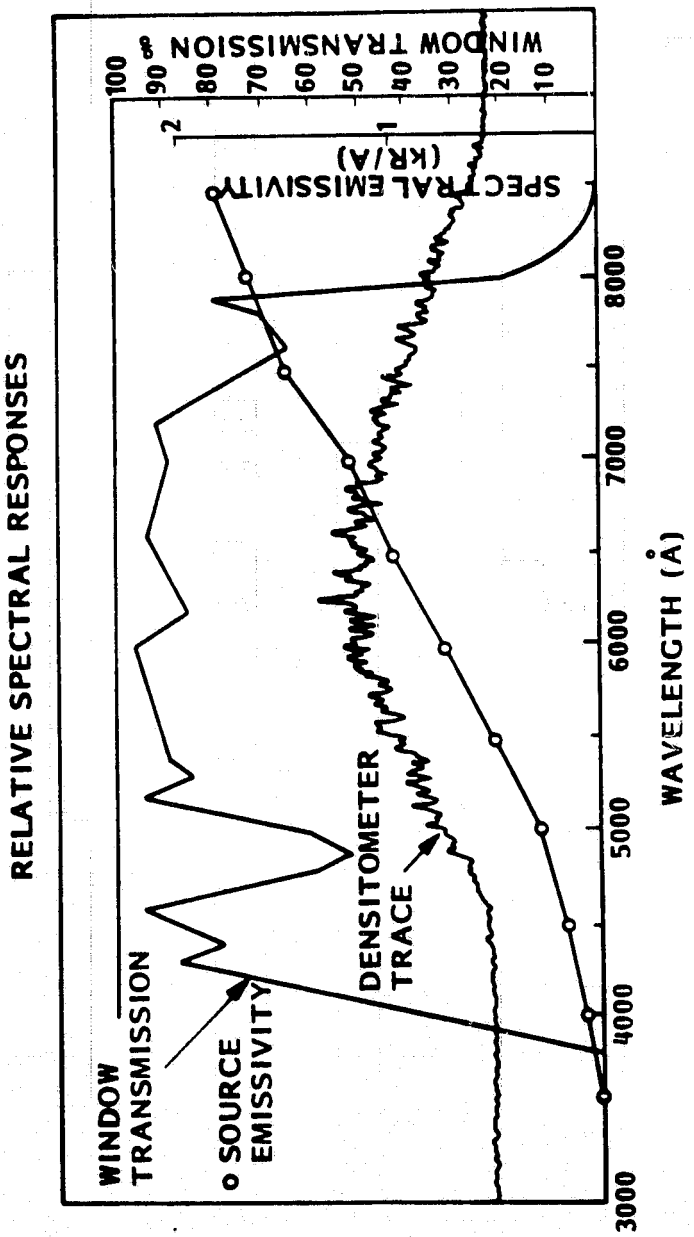

Figure 3.

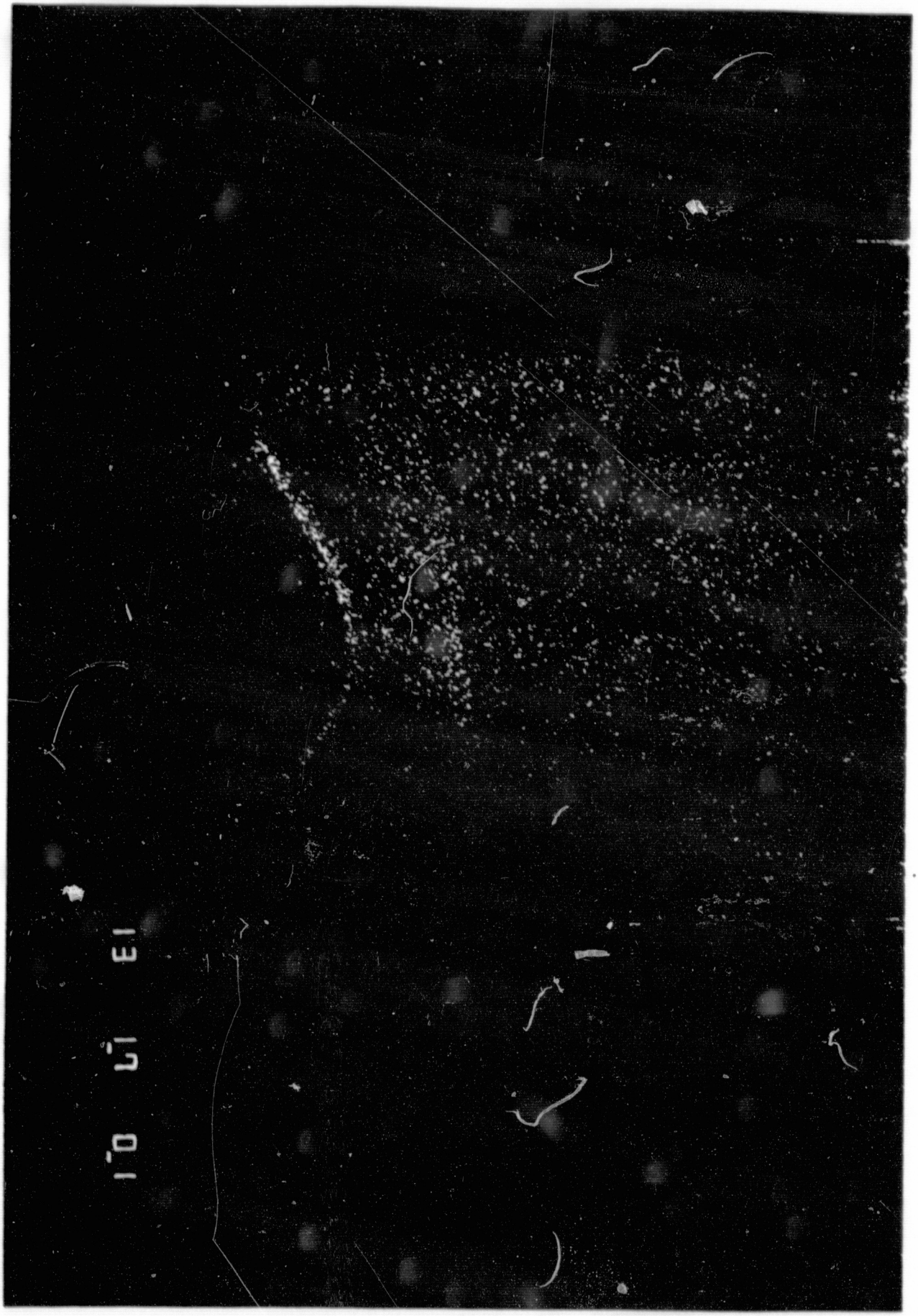

Figure 5a.

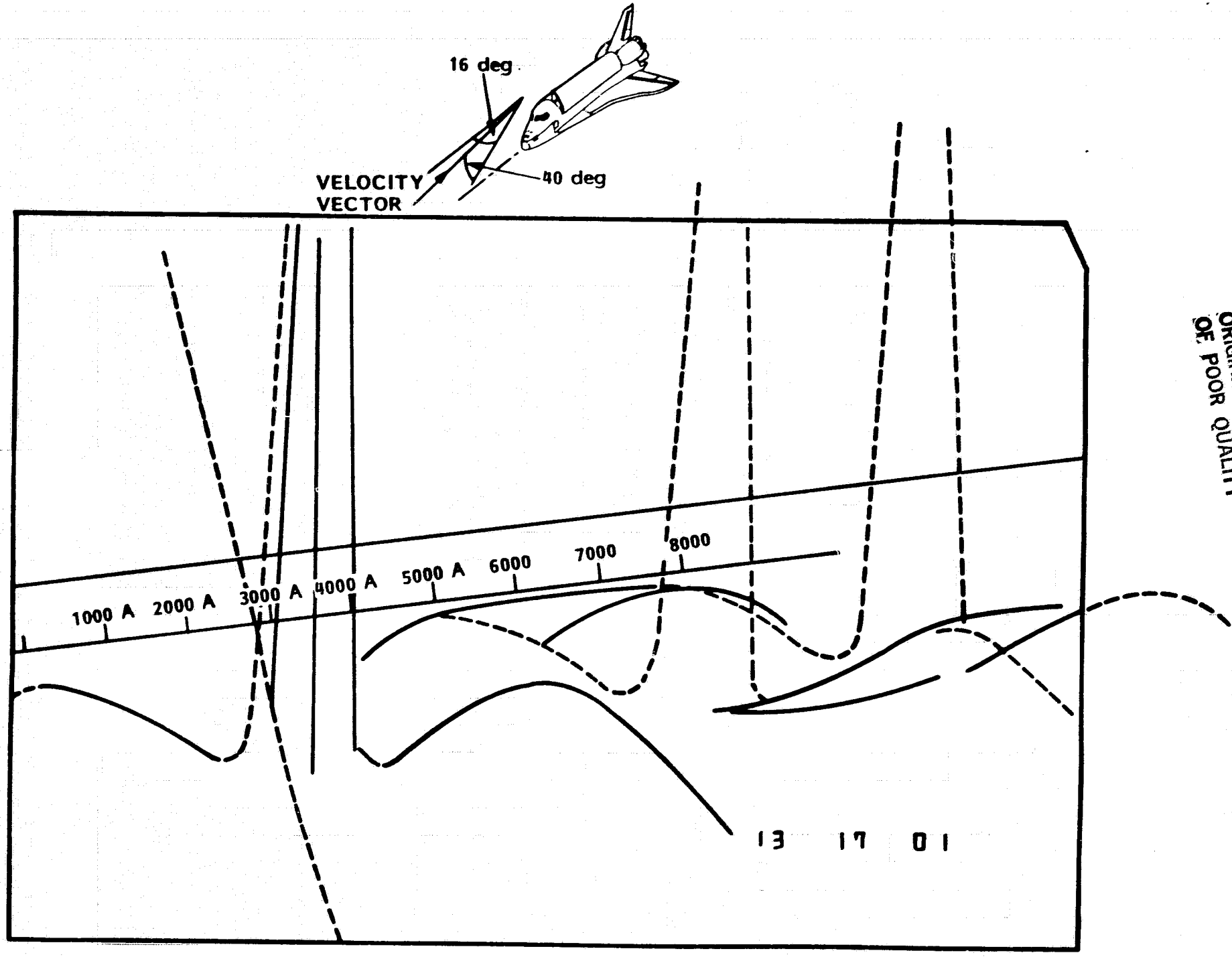

Figure 5b

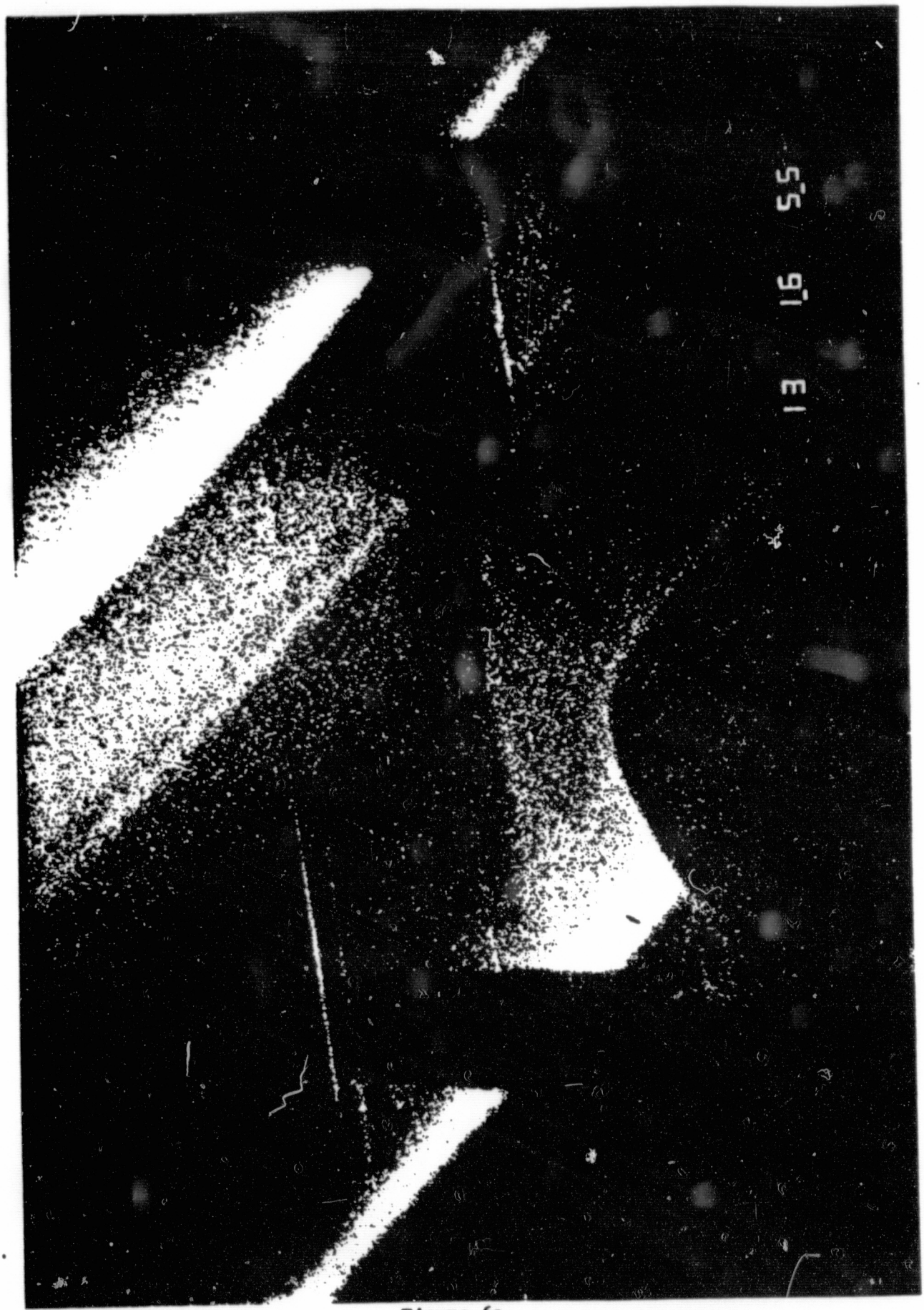

Figure 6a.

Figure 8a.

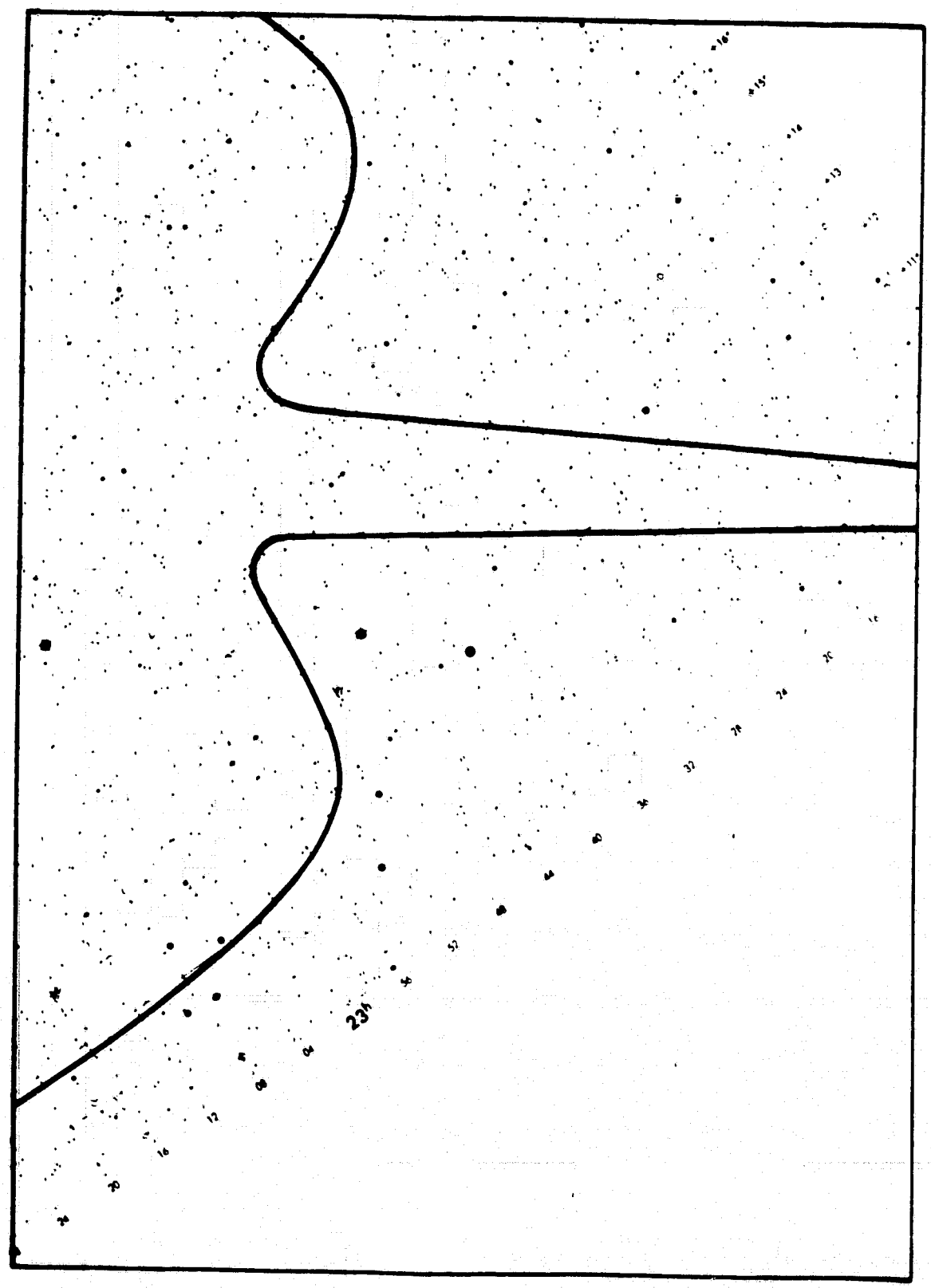

Figure 8b.

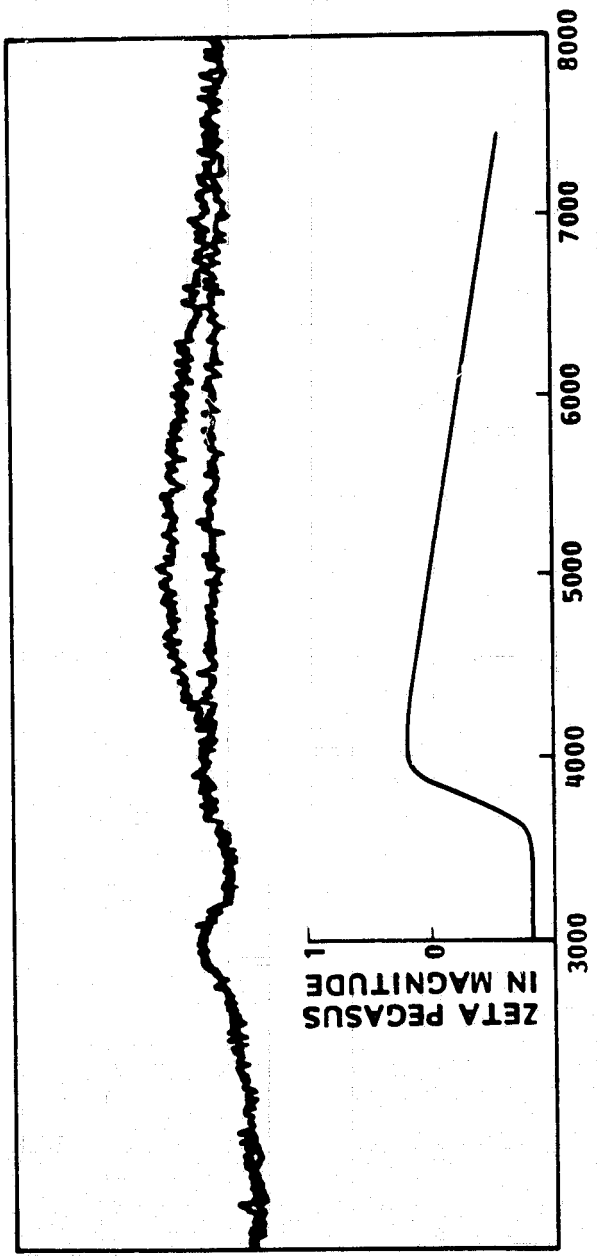

Figure 9.